Title: A standardized surgical technique for rat superior cervical ganglionectomy

Authors: Luis Emilio Savastano, Analía Elizabeth Castro, Marcos René Fitt, Martin Fredensborg Rath, Horacio Eduardo Romeo, Estela Maris Muñoz

PII: S0165-0270(10)00361-4
DOI: doi:10.1016/j.jneumeth.2010.07.007
Reference: NSM 5682

To appear in: *Journal of Neuroscience Methods*

Received date: 3-5-2010
Revised date: 5-7-2010
Accepted date: 7-7-2010

Please cite this article as: Savastano LE, Castro AE, Fitt MR, Rath MF, Romeo HE, Muñoz EM, A standardized surgical technique for rat superior cervical ganglionectomy, *Journal of Neuroscience Methods* (2008), doi:10.1016/j.jneumeth.2010.07.007

RESEARCH ARTICLE

A standardized surgical technique for rat superior cervical ganglionectomy

Authors: Luis Emilio Savastano[1], Analía Elizabeth Castro[1], Marcos René Fitt[1], Martin Fredensborg Rath[2], Horacio Eduardo Romeo[3] & Estela Maris Muñoz[1]

[1] Institute of Histology and Embryology of Mendoza (IHEM), School of Medicine, National University of Cuyo, Mendoza; National Council of Scientific and Technical Research (CONICET), National Agency for the Promotion of Science and Technology (ANPCyT), Argentina.

[2] Department of Neuroscience and Pharmacology, Panum Institute, University of Copenhagen, Copenhagen, Denmark.

[3] Pontificia Universidad Católica Argentina, Facultad de Ciencias Médicas, PIB-CONICET, Buenos Aires, Argentina.

Number of:

- **Pages: 51**
- **Figures: 3**
- **Tables: 3**
- **Supplementary videos: 14**

Corresponding author: Luis E. Savastano, M.D., Parque General San Martin, CC: 56, Mendoza, Argentina, CP: 5500. Phone: 54-261-4135000 (2716); Fax: 54-261- 4494117. Email: savastanoluis@hotmail.com

Authors

- **Luis Emilio Savastano, MD** (corresponding author)
  - Postal address: IHEM/CONICET
    Facultad de Ciencias Médicas. UNCuyo
    Parque Gral. San Martín, CC 56
    Mendoza (5500), Argentina
  - Email: savastanoluis@hotmail.com
  - Telephone number: 54-261-4135000 (Int. 2716)
  - Fax number: 54-261-4494117

- **Analía Elizabeth Castro, PhD student**
  - Postal address: IHEM/CONICET
    Facultad de Ciencias Médicas. UNCuyo
    Parque Gral. San Martín, CC 56
    Mendoza (5500), Argentina
- **Marcos René Fitt, Medicine student**
  - Postal address: IHEM/CONICET
    Facultad de Ciencias Médicas. UNCuyo
    Parque Gral. San Martín, CC 56
    Mendoza (5500), Argentina
- **Martin Fredensborg Rath, PhD**
  - Postal address: Department of Neuroscience and Pharmacology
    University of Copenhagen
    Panum Institute 24.3
    Blegdamsvej 3
    DK-2200 Copenhagen, Denmark
- **Horacio Eduardo Romeo, PhD**
  - Postal address: Facultad de Ciencias Médicas
    Pontificia Universidad Católica Argentina
    Av. Alicia Moreau de Justo 1500 (4to piso)
    C1107AFD Ciudad de Buenos Aires,
    Argentina

- **Estela Maris Muñoz, PhD**
  - Postal address: IHEM/CONICET
    Facultad de Ciencias Médicas. UNCuyo
    Parque Gral. San Martín, CC 56
    Mendoza (5500), Argentina

RESEARCH HIGHLIGHTS

1. SCGx as a valuable model to study homeostatic regulation and nerve injury and recovery.
2. The rat`s neck offers anatomical landmarks to approach, identify and remove the SCG.
3. SCGx can be performed with or without muscle injury.
4. Decentralization and denervation as alternatives to disrupt the sympathetic pathway.

Abstract

Superior cervical ganglionectomy (SCGx) is a valuable microsurgical model to study the role of the sympathetic nervous system in a vast array of physiological and pathological processes, including homeostatic regulation, circadian biology and the dynamics of neuronal dysfunction and recovery after injury. Despite having several experimental applications in the rat, a thorough description of a standardized procedure has never been published. Here, we provide a brief review of the principal features and experimental uses of the SCGx, the surgical anatomy of the neck and sympathetic cervical chain, and a step-by-step description of how to consistently remove the superior cervical ganglia through the omohyoid muscle or the carotid triangle. Furthermore, we suggest procedures and precautions to be taken during and after surgery to optimize results and describe tools to validate surgical success. We expect that the following standardized and optimized protocol will allow researchers to organize knowledge into a cohesive framework in those areas where the SCGx is applied.

Keywords: Superior cervical ganglia; Superior cervical ganglionectomy; Cervical sympathectomy; Denervation; Decentralization; Surgical procedure; Rat.

Abbreviations

AA-NAT: arylalkylamine N-acetyltransferase; **aDM**: anterior belly of the digastric muscle; **CB:** carotid body; **CBA:** carotid body artery; **CCA**: common carotid artery; **CT**: carotid triangle; **DCF**: deep cervical fascia; **DM**: digastric muscle; **ECA**: external carotid artery; **ECN:** external carotid nerve; **ECNx:** external carotid nerve section; **EJV**: external jugular vein; **HN**: hypoglossal nerve; **ICA**: internal carotid artery; **ICN:** internal carotid nerve; **ICNx:** internal carotid nerve section; **IJV:** internal jugular vein; **LFV:** linguofacial veins; **MM:** masseter muscle; **NE:** norepinephrine; **OA:** occipital artery; **OHM**: omohyoid muscle; **PBS**: phosphate buffered saline; **pDM**: posterior belly of the digastric muscle; **SCF**: superficial cervical fascia; **SCG:** superior cervical ganglia; **SCGx:** superior cervical ganglionectomy; **SCN:** suprachiasmatic nuclei; **SCNx:** suprachiasmatic nuclei lesion; **SHM**: sternohyoid muscle; **SMM**: sternomastoid muscle; **ST:** sympathetic trunk; **STx:** sympathetic trunk section; **VN**: vagus nerve.

1. Introduction

Understanding the physiological mechanisms that regulate the internal environment is a major challenge for both physicians and scientists. Although several animal models have been developed to study the role of the sympathetic nervous system in homeostatic regulation, the rat has become the preferred experimental species, replacing larger animals (Jänig and Häbler, 2003). Removal of the superior cervical ganglia (SCG), namely superior cervical ganglionectomy (SCGx), was introduced in rats more than 50 years ago (Ifft, 1953) and now represents a valuable microsurgical model in autonomic nervous system research (Romeo et al., 1986; 1990; 1991a; Stehle et al., 1993; Møller et al., 1997; Rath et al., 2006; Muñoz et al., 2007; Rath et al., 2009). Despite the numerous applications of SCGx, the procedure has never been methodically described in the rat, and a standardized surgical technique is still missing in the literature.

The SCG are the uppermost ganglia of the paravertebral sympathetic chain; in rats, each ganglion contains 13000-45000 neurons, weighs 1 mg and has a volume of ~0.5 mm^3 (Smolen et al., 1983; Ribeiro et al., 2004). Within these well-defined structures, the preganglionic input fibers ascending in the sympathetic trunk (ST) synapse with the postganglionic neurons which innervate the neck, face and intracranial structures, mainly via the external and internal carotid nerves (ECN and ICN) (Cardinali and Romeo, 1991). The SCG's field of innervation includes the pineal gland, hypophysis and median eminence, carotid body (CB), the thyroid and parathyroid glands, the iris and eye lid (Cavallotti et al., 2005). The Müller's muscle, which controls the position of the

upper eyelid, is partly innervated by the homolateral sympathetic system through the ICN. Any interruption of the sympathetic pathway to the eye makes this muscle weak, resulting in blepharoptosis (drooping of the upper eyelid) (Cardinali and Romeo, 1991). This phenomenon is used as indicator of the successful removal of the SCG.

The physiological activities of the SCG postganglionic neurons on the peripheral target tissues are mainly accomplished through norepinephrine (NE) released from their nerve terminals (Cardinali and Romeo, 1991). Several neuropeptides produced by these neurons have also been shown to play physiological roles in the innervated tissues, such as the neuropeptide Y in the pineal gland (Reuss and Moore, 1989; Benarroch, 1994; Klimaschewski et al., 1996; Zigmond, 2000; Møller et al., 2002). The concentration of NE in the synaptic cleft is under the control of different mechanisms, such as simple diffusion and uptake into nerve terminals or other cells in the vicinity, followed by intracellular metabolism. The presynaptic uptake plays an important role in terminating the synaptic stimulus, and in the removal and inactivation of circulating catecholamines (Iversen, 1971).

The SCG's innervation territory described above, together with the hormone-dependent ganglion activity, makes the SCGx a key model in the study of peripheral sympathetic innervation in neuroendocrine interactions (Cardinali and Romeo, 1991; Cardinali and Stern, 1994). Indeed, the SCGx has been employed to investigate how light and the circadian clock influence neuroendocrine functions, e.g. circadian melatonin synthesis in the rat pineal gland. Under the control of the hypothalamic suprachiasmatic nuclei (SCN), NE is released in the pineal gland from both ICN at night, and modulates the

melatonin rhythm-generating enzyme, the arylalkylamine N-acetyltransferase (AA-NAT) (Klein, 2007). In rats, the 150-fold and 50-70-fold increase in nocturnal AA-NAT expression and activity, respectively, induces a 10-fold rise in the synthesis and secretion of melatonin (Borjigin et al., 1995; Roseboom et al., 1996; Perreau-Lenz et al., 2005). This remarkable dynamics has turned the melatonin rhythm into one of the preferred output markers of the circadian clock (Weaver, 1998). Even though circulating catecholamines released during stress may stimulate denervated pinealocytes (Parfitt and Klein, 1976; Lynch et al., 1977), the establishment and maintenance of the circadian melatonin rhythm depend on the sympathetic innervation of the pineal gland from both SCG (Klein et al., 1971). In rat pineal gland, AA-NAT mRNA becomes rhythmic at postnatal day 5, when sympathetic nerve fibers penetrate into the pineal parenchyma, causing an evident day-to-night difference of melatonin from postnatal day 11 throughout the animal life (Maronde and Stehle, 2007; Yamazaki et al., 2009). Interestingly, pineal glands transplanted into different locations survive and exhibit active secretory processes, indicating sympathetic reinnervation of the grafts. Nevertheless, day-to-night differences in circulating melatonin are only restored following transplants into the anterior eye chamber, where SCG postganglionic fibers that innervate the iris are present, suggesting that the restoration of the circadian melatonin rhythm depends on the graft reinnervation by the host SCG (Wragg et al., 1967; Moore, 1975; Bäckström et al., 1976; Lingappa and Zigmond, 1987; Wu et al., 1993). Nocturnal increase of AA-NAT activity in pineal glands transplanted into the anterior eye chamber is abolished after SCG removal (Bäckström et al., 1976), but is not affected by a brief light exposure in the late dark period, in contrast to the significant decrease of AA-

NAT activity in control animals (Lingappa and Zigmond, 1987). Functional differences between pineal glands *in situ* and those transplanted into the anterior eye chamber suggest the involvement of at least two different populations of sympathetic neurons within the SCG.

Even though several experimental models have been developed to disrupt the melatonin circadian system (Moore and Klein, 1974; Zigmond et al., 1981; Perreau-Lenz et al., 2003), the bilateral SCGx has proved to be a solid and reliable procedure to completely prevent nocturnal AA-NAT increase, irreversibly suppressing melatonin rhythmicity and all trans-synaptic sympathetic influence on the pineal gland (Klein et al., 1971; Møller and Baeres, 2002). The defined anatomy of the SCG and its branches also allows decentralization or denervation by lesioning pre and postganglionic axons, respectively (Taxi and Eugène, 1995); each lesion causes specific effects on the melatonin rhythm (Zigmond et al. 1981; Zigmond et al. 1985). SCG-related procedures are preferred to central nervous system interventions, such as a suprachiasmatic nuclei lesion (SCNx), because the latter are technically demanding and interpretations of results are complicated by the disruption of a wide array of behavioral and physiological rhythms and the overlapping aftereffects of intracranial surgery.

The SCGx has also enhanced our knowledge of neuroimmunomodulation (Esquifino and Cardinali, 1994; Elenkov et al., 2000; Nance and Sanders, 2007). Noradrenergic fibers originating from the SCG innervate the cervical lymph nodes (Romeo et al., 1994) and the thymus, modulating lymphocyte proliferation, migration, and differentiation (Ramaswamy et al., 1990), and regulate inflammation and tissue repair through

submandibular gland factors (Mathison et al., 1994). Moreover, the SCGx has become a recognized model to investigate the role of the sympathetic nervous system in bone remodeling (Boggio et al., 2004; Haug and Heyeraas, 2006), carcinogenesis (Romeo et al., 1991b; Raju et al., 2007), and brain vasculature pathophysiology (Nagao et al., 1992; May and Goadsby, 1999; Coutard et al., 2003), and SCGx is considered a potential procedure to unravel pain-generating mechanisms (Perl, 1999; Wasner et al., 2003; Gibbs et al., 2008).

SCGx has shown itself to be a useful model to study both sympathetic deprivation and stimulation. Based on the Wallerian or anterograde degeneration paradigm, varying neuroendocrine consequences of SCG removal should be expected (Emmelin and Trendelenburg, 1972). If the sequelae of SCGx are examined a week or more after the surgery (chronic SCGx), the results obtained would correspond to sympathetic deprivation. However, if the consequences of ganglionectomy are evaluated on the first few days following surgery (acute SCGx), during the early anterograde degeneration that takes place with short latency, a temporary supraliminal release of neurotransmitter from the degenerating varicosities might cause a transient increase in postsynaptic activity. The time frame is variable (~1-3 days) depending on the innervated tissue, and it is believed to be proportional to the length of the distal stumps of the lesioned postganglionic axons (Cardinali and Romeo, 1991).

The SCGx has been developed in a broad range of animal species, but to our knowledge, a straightforward surgical protocol in rat has not yet been published. To achieve reproducible results and assure laboratory animal welfare, a standardization of the SCGx is needed. Hedger and Webber (1976) and Weijnen et al. (2000) provided thorough descriptions of the sympathetic

cervical chain with excellent illustrations of the main vascular and nervous structures of the upper neck; however, the anatomical landmarks required to reach the SCG and its branches were not described in detail. In consequence, a surgical anatomy of the region where the SCG is located is needed to achieve a consistent cervical sympathetic disruption with minimal animal morbimortality.

In this protocol, we present a photo series of the dissection of an exsanguinated rat's neck, and describe step-by-step the surgical technique (illustrated by photographs and videos) for reliable removal of the SCG. Moreover, we introduce technical modifications to make the procedure more precise, less invasive and highly reproducible. We also present some complementary tools to evaluate surgical performance. It is our expectation that researchers who are interested in incorporating the SCGx as a routine technique in their laboratories will find the required information to succeed in this report.

2. Materials and methods

2.1. Animals

Surgical procedures were performed on adult Wistar rats (3 to 5 months old) weighing 250 to 350 g. Male and female rats were used for photography and video production. Nevertheless, animal gender, age and strain must be chosen according to the specific aims of each study. Animals were housed individually in a temperature and humidity controlled room and kept on a 12:12-hours light:dark cycle. The animals were allowed free access to food and water. Adequate measures were taken to minimize pain and discomfort taking into account human endpoints for animal suffering and distress. Our experiments were carried out in accordance with the National Institutes of Health Guide for the Care and Use of Laboratory Animals. The protocol presented here was approved by the Institutional Animal Care and Use Committee, National University of Cuyo, Mendoza, Argentina.

2.2. Reagents

2.2.1. Dissection of the neck and SCGx

- Ketamine (50 mg kg^{-1}; e.g. Wyeth, cat. no. 206205-01)
- Xylazine (5 mg kg^{-1}; e.g. Lloyd Laboratories, cat. no. 139-236)

Other anesthetic regimens may be considered according to the aims of the study to avoid interactions between the anesthetic and the experimental protocol.

- Ocular surface protecting lubricant
- 5% benzalkonium chloride solution
- Povidone-iodine solution
- 0.9% (w/v) NaCl

2.2.2. Immunohistochemistry

- 4% paraformaldehyde in phosphate buffered saline (PBS)
- Histoplast (Biopack)
- Monoclonal anti-neurofilament antibody (BIOMOL International, cat. no. NA1225)
- Monoclonal anti-tyrosine hydroxylase antibody (Sigma-Aldrich®, cat. no. T2928, clone TH-16)
- Biotinylated anti-mouse IgG (H+L) (Vector Laboratories, cat. no. BA-2001)
- Fluorescein streptavidin (Vector Laboratories, cat. no. SA-5001)
- Texas Red® streptavidin (Vector Laboratories, cat. no. SA-5006)
- ProLong® Gold antifade reagent with DAPI (Invitrogen™, cat. no. P-36931).

2.3. Equipment

2.3.1. Dissection of the neck and SCGx

- Hudson microdissecting forceps (e.g. Roboz Surgical Instruments, cat. no. RS-5237)
- Adson microdissecting forceps 1 x 2 teeth (e.g. Roboz Surgical Instruments, cat. no. RS-5233)
- Two microdissecting tweezers, pattern no. 7 (e.g., Roboz Surgical Instruments, cat. no. RS-5047)
- Microdissecting spring scissors (e.g. Roboz Surgical Instruments, cat. no. RS-5601)
- Microdissecting scissors (e.g. Roboz Surgical Instruments, cat. no. RS-5882)
- Operating scissors (e.g. Roboz Surgical Instruments, cat. no. RS-6814)
- Self-retaining microdissecting retractor (e.g. Roboz Surgical Instruments, cat. no. RS-6561)
- Halsted mosquito hemostat (e.g. Roboz Surgical Instruments, cat. no. RS-7101)
- Needle holder (e.g. Roboz Surgical Instruments, cat. no. RS-7830)
- 4-0 nylon on 20-mm needle (e.g. Surgikal®, cat. no. 5420)
- Saline-moistened cotton Q-tips
- Seven staples: 1 big (upper incisors), 2 medium (neck`s cushion) and 4 small size (limbs)

- Gauze
- Small animal clipper
- Styrofoam pad
- Surgical cloth
- Latex gloves
- Face mask
- Surgical binocular microscope (Leitz Wetzlar)
- Peristaltic pump (NEMI Scientific, Inc Model 610)
- Sterilizer (e.g. Germinator 500 System, Cell Point Scientific, Inc.)

2.3.2. Immunohistochemistry

- Microm HM 325 Microtome
- Olympus FV 1000 Confocal Microscope.

2.4. Dissection of the neck

Under ketamine/xylazine anesthesia, the animals were perfused transcardially with ~70 ml of 0.9% saline solution. The perfusion was performed with a peristaltic pump after placing a cannula in the left ventricle. Blood and the saline solution were drained through an incision in the right atrium. Fixative solution was not used, in order to maintain the elastic properties of the nerves, vessels and muscles.

Exsanguinated rats were placed in a dissection tray and the superficial anatomical landmarks of the ventral neck region were identified by palpation. A 4-cm vertical incision was performed and the skin retracted. The superficial cervical fascia (SCF) was removed, the mandibular glands and external jugular veins (EJV) were dissected, and the superficial muscles of the ventral neck were examined. The cranial portion of the sternomastoid muscle (SMM) and the omohyoid muscle (OHM) were transected. The deep cervical fascia (DCF) and carotid sheath were partially removed to expose the common carotid artery (CCA), the internal jugular vein (IJV) and the vagus nerve (VN). The CCA was bluntly dissected up to the level of its bifurcation into the external and internal carotid arteries (ECA and ICA). The SCG was identified behind the carotid bifurcation and freed of fat and connective tissue. The occipital artery (OA) was removed and the nervous branches emerging from the ganglion were dissected up to ~5 mm. During the procedure, photos were taken using a standard digital camera (Casio EX-Z70); the images were edited with Adobe Photoshop CS3 and Power Point Microsoft Office 2007.

2.5. SCGx

Under ketamine/xylazine anesthesia, the ventral neck region was shaved and disinfected. The salivary glands were exposed through a 2.5-cm vertical incision and retracted to expose the underlying muscles. Two alternative strategies to approach and remove the SCG were optimized. In the first one, after sectioning the OHM and cranially dissecting the CCA, the SCG were identified behind the carotid bifurcations and then gently pulled until their avulsion. This technique, commonly used in several laboratories, was named by

us as the classical technique. In the second one, the carotid bifurcations were identified through the carotid triangles (CT) and the SCG were removed after sectioning the ST, ECN and ICN. The later procedure is introduced here for the first time, and therefore, it was named innovative technique. Notably, this surgical approach exposes SCG branches and allows operators to perform other SCG-related procedures, such as decentralization by injuring the ST, and denervation by lesioning either ECN or ICN. After SCG removal, the skin was closed with nylon sutures. The main surgical steps were recorded using a digital camera (Casio EX-Z70) and a video camera (Sony HDV-SX1). Images were edited with Adobe Photoshop CS3 and Power Point Microsoft Office 2007; video edition was performed using Adobe CS3 Video Workshop.

2.6. Immunohistochemistry

After removal, the SCG were fixed in 4% paraformaldehyde in PBS overnight at 4°C. The ganglia were washed three times in PBS for 5 minutes per wash, dehydrated in increasing concentrations of ethanol (70, 80, 96, 100%) and washed twice in xylene for 5 minutes each, and finally embedded in Histoplast (Biopack). Five µm sections from fixed ganglia were cut using a Microm HM-325 microtome. Immunohistochemical detection of the neurofilament protein and the enzyme tyrosine hydroxylase was performed as previously described (Semino-Mora et al., 2003). After deparaffinization and hydration, the slides were boiled in 0.1M citrate buffer pH 6 for 30 minutes in a pressure cooker and then washed three times in PBS for 5 minutes each. Non-specific labeling was blocked by incubating SCG sections in blocking solution (50 mM Tris-HCl pH 7.3, 0.125 M NaCl, 5% v/v normal horse serum, 20 mg/ml

bovine serum albumin, fraction V, and 5 mg/ml standard whole milk powder) for 30 minutes at room temperature in a covered humid chamber. Immunodetection was performed using monoclonal primary antibodies diluted in the blocking solution without normal horse serum (anti-neurofilament antibody: dilution 1:400, BIOMOL International; anti-tyrosine hydroxylase antibody: dilution 1:100, Sigma-Aldrich®). Sections were incubated overnight at 4°C and then washed three times for 5 minutes each in Tris-buffered saline with 0.05% Tween-20. The bound primary antibodies were detected using a biotinylated anti-mouse antibody (dilution 1:300, Vector Laboratories) for 2 hours at room temperature. After three washes, sections were incubated for 1 hour at room temperature with fluorescein streptavidin and Texas Red® streptavidin (dilution: 1:200, Vector Laboratories) for the neurofilament protein and the enzyme, respectively. After being washed three times, SCG sections were mounted in ProLong® Gold antifade reagent with DAPI (Invitrogen™). The sections were examined using an Olympus FV-1000 confocal microscope; images were edited with Adobe Photoshop 6.0.

3. Results

3.1. Surgical anatomy of the neck

A photo series of the dissection of an exsanguinated rat's neck is shown in Figure 1. The *regio intermandibularis* was identified between the two mandibular branches, and the *regio presternalis* was located cranially to the manubrium of sternum (Fig. 1A). After cutting and reflecting the skin that covers the ventral side of the neck, the SCF was identified as a yellow-pinkish connective tissue layer (Fig. 1B). The mandibular and sublingual salivary glands, lymph nodes and the superficial layer of muscles were exposed after SCF removal (Fig. 1C). The mandibular glands were identified as a pair of large, elongated oval glands lying in the mid-ventral neck area, with some lymph nodes at their anterior borders. Wharton`s salivary duct was observed as a yellow-gray tubular structure coming from the cranial end of the mandibular gland and passing ventrally between the masseter muscle (MM) and the anterior belly of the digastric muscle (aDM). The sublingual glands were located upon the lateral surface of the mandibular glands. Underneath the mandibular glands and laterally from the SMM, the EJV were identified as long and thick vessels, with several branches draining blood from the face, jaw and neck (Fig. 1D).

After displacing the mandibular glands laterally, the superficial layer of muscles of the ventral neck was exposed (Fig. 1E). The sternohyoid muscles (SHM) were identified as two muscular bands running along the mid-ventral line of the neck, from the manubrium of sternum to the lower border of the hyoid. The SMM were observed as elongated muscular bands aligned diagonally from

their insertion point in the sternum to the lateral sides of the neck. The OHM were identified laterally from the SHM and underneath the SMM. The posterior part of the digastric muscles (pDM) extended caudally from the hyoid to the occipital bone, whereas the aDM were localized in the *regio intermandibularis*, running parallel to the mid-ventral line. The anatomical landmarks named CT were identified in the lateral regions of the neck, bordered by the OHM (medially), SMM (caudally and laterally) and pDM (cranially and laterally) (Fig. 1F).

The resection of the OHM and SMM uncovered the carotid sheath (Fig. 1G). This fibrous tissue derived from the DCF, enclosed the CCA, IJV and VN. Some cervical lymph nodes were usually observed as small bean-shaped, reddish-yellow bodies loosely attached to the carotid sheath. The removal of the carotid sheath revealed the CCA (medially), VN (laterally) and IJV (posteriorly) (Fig. 1H). The Y-shaped bifurcation of the CCA into the ECA and ICA was usually observed downwards and medially from the mandibular angular process, a bone tip easily palpable at the ventrolateral region of the upper neck. The ECA was the medial and superficial branch that emerged from carotid bifurcation, whereas the ICA ran deeper and laterally. The OA was identified as a branch of the ECA that crossed over the SCG, ICA and VN towards the lateral side of the neck (Fig. 1H). The SCG, located dorsally to the OA and embedded in fat and connective tissue, was closely applied to the CCA bifurcation. The removal of this soft connective tissue and the OA, and the retraction towards the neck mid-line of the ECA completely exposed the SCG (Fig. 1I).

The SCG presented considerable interindividual variability in size (up to ~50 %) and shape (ranging from oval to slightly resembling a triangle), although

this structure was usually identified as a spindle-shaped glassy reddish-gray structure, ~3 mm in length and ~0.5 mm^3 in volume. The ICN originated from the cranial pole of the SCG and followed the ICA into the carotid canal. The ECN usually emerged from the medial side of ganglion and then run parallel to the ECA. The ST entered through the caudal pole of the SCG after running underneath the main cervical blood vessels. Other thinner branches arising from the SCG were occasionally observed. The VN, running alongside the lateral side of the CCA and ICA, was identified as a shining white strand with a spindle-shaped enlargement in its cranial portion (the nodose ganglion). Underneath the pDM, the hypoglossal nerve (HN) was observed as a shining white strand crossing over the ICA, just medially from the mandibular angular process.

3.2. SCGx

The surgical procedure should be carried out by operators trained in the use of laboratory animals. Before SCGx, we recommend that the researcher performs neck dissections on euthanized animals to become familiar with the regional anatomy. Both the classical and an innovative surgical technique for SCG removal are thoroughly described below. The reader can find a photo series that summarizes the main steps of both procedures in Figure 2. Supplementary videos are also provided.

Preoperative setup

1. Place the sterile surgical instruments on a Styrofoam pad. Use latex gloves and a face mask to keep the surgical field reasonably aseptic.

2. Weigh animals accurately to determine the doses of anesthetics to be used.
3. Anesthetize the rat with i.p. ketamine (50 mg kg^{-1}) and xylazine (5 mg kg^{-1}) mixed in the same syringe.
4. Apply an ocular surface protecting lubricant to prevent corneal dehydration and ulceration.
5. Monitor the intensity of anesthesia by foot pinch.
6. Shave the ventral side of the neck using an animal clipper.
7. Place the animal on the Styrofoam pad on its back, with the head located towards the operator. Place the animal`s neck over a cushion (e.g. two medium staples), and hold its limbs with smaller staples. Stretch the animal`s neck by pulling on the upper incisors with the biggest staple and gently pull out the tongue to assure an adequate airway (see Supplementary Video 1 online).
8. Rinse the skin with 5% benzalkonium chloride solution.

Incision and salivary gland dissection

9. Use the operating scissors to make a ~2.5 cm mid-line skin incision in the ventral side of the neck, from the *regio intermandibularis* to the *regio presternalis* (Figs. 2A-B) (see Supplementary Video 2 online).

   ! CAUTION The glandular tissue and the branches of the linguofacial veins (LFV) located at the level of the chin should not be damaged.
10. Retract the cut edges of the skin to adequately expose the superficial cervical fascia (SCF) and the underlying mandibular salivary glands (Figs. 2B-C) (see Supplementary Video 3 online).

11. Cut the soft connective tissue at the level of the mid-line, between the left and right mandibular glands (Fig. 2C) (see Supplementary Video 4 online).

? TROUBLESHOOTING (see Table 1)

12. Lift up the mandibular glands and cut medially the translucent sheets of connective tissue that bind the glands to the SHM, SMM and DM (Figs. 2D-E) (see Supplementary Video 5 online).

! CAUTION During this step, the EJV and Wharton`s duct are exposed. Damage to these structures can cause complications from severe bleeding and saliva leakage from the wound with delayed scarring and local infections.

13. Retract the skin and mandibular glands laterally using a self-retaining microdissecting retractor (Fig. 2E) (see Supplementary Video 6 online).

! CAUTION The EJV must not be retracted.

SCG identification and removal

The following steps may be performed under direct vision or, preferably, using a magnifying instrument. The neck must be positioned properly as shown in Supplementary Video 1.

14. Expose the CCA, identify the SCG and remove it. Two different strategies to perform this step are described here:

CLASSICAL TECHNIQUE

A. Transect the OHM longitudinally to expose the CCA and its bifurcation (Figs. 2E-F) (see Supplementary Video 7 online).

▲CRITICAL STEP

i. Using Q-tips, push the SMM laterally and the SHM medially. The CCA can be identified as a pulsating dark red vessel below the OHM that gives rise to a beating area in the muscle.

? TROUBLESHOOTING

ii. Use microdissecting spring scissors to create a hole in the OHM medially from the beating area, and extend the muscular section cranially. The thin venous branches and nerves should not be cut during the OHM section.

! CAUTION If the hole is made over the beating area, massive bleeding due to CCA injury may occur.

iii. Using Q-tips, retract the cut edges of the OHM to open the muscular incision and expose the CCA running alongside the lateral face of the VN.

iv. Follow the CCA cranially until its bifurcation.

? TROUBLESHOOTING

B. Expose and identify the SCG (Fig. 2G) (see Supplementary Video 8 online).

i. Use microdissecting tweezers to turn over the ECA.

! CAUTION Arteries must be held indirectly by the surrounding connective tissue to avoid tearing and profuse hemorrhage. Additionally, arterial compression can cause thrombosis due to endothelial injury.

! CAUTION SCG removal should not be attempted via a ventral to dorsal approach through the carotid bifurcation.

This strategy may injure the carotid body (CB), located close to the ICA, and may rupture the OA and the carotid body artery (CBA) leading to profuse bleeding.

ii. Identify the SCG medially from the carotid bifurcation.

▲CRITICAL STEP Expose the ganglion with the tips of the tweezers via delicate and precise movements.

? TROUBLESHOOTING

! CAUTION During the training period the SCG may be confused with the VN, nodose ganglion, lymph nodes and HN. If the vagus nerves are seriously damaged, the animal will die from asphyxia.

C. Pull the SCG until its avulsion (see Supplementary Video 9 online).

▲CRITICAL STEP

i. Use the tweezers to tightly hold the distal end of the SCG.

ii. Pull the ganglion until the carotid nerves and the ST are successively torn. Traction must be performed with constant strength, slowly and gently during ~30 seconds, up and towards the animal`s tail.

! CAUTION Excessive SCG traction may cause unexpected ganglion rupture and massive bleeding due to carotid artery damage. If a nerve branch offers resistance, cut it with scissors.

INNOVATIVE TECHNIQUE

A. Locate the beating area of the ECA through the DCF that covers the CT (Fig. 2E) (see Supplementary Video 10 online).

? TROUBLESHOOTING

B. Use a Halsted mosquito hemostat to retract and maintain the ECA laterally. This action allows the operator to use both hands in the following steps (see Supplementary Video 11 online).

C. Create a hole in the DCF medially from the ECA (Figs. 2F') (see Supplementary Video 12 online).

D. Identify the SCG medially from the carotid bifurcation (Fig. 2G').

E. Hold the SCG by the ST and release its nervous branches from the carotid sheath with the tip of a tweezers. If too much resistance is noted, carefully cut the tough connective tissue with a pair of scissors (see Supplementary Video 13 online).

F. Cut the preganglionic and postganglionic branches and remove the SCG (see Supplementary Video 14 online).

i. Using microdissecting tweezers, delicately stretch the ganglion`s branches.

ii. Use microdissecting spring scissors to successively cut the ST, ECN and ICN ~3 mm from the ganglion.

▲CRITICAL STEP Remove the connective tissue surrounding pre and postganglionic nerves in order to be certain that they will be actually sectioned at a level where neuronal perikarya are absent.

! CAUTION Other nerve branches from the SCG have been described (Hedger and Webber, 1976). They may be cut to remove the ganglion completely.

iii. Harvest the intact SCG.

NOTE: The innovative approach allows operators to perform decentralization and denervation by nerve sectioning, crushing, freezing or ligation (Zigmond et al., 1985; Taxi and Eugène, 1995). In experiments with long survival times (i.e., 1 month or longer), a large piece of the nerve may be removed to avoid reinnervation of the denervated tissues. To decentralize the SCG, the cervical ST should be cut ~3 mm before its entry into the ganglion and again more caudally, removing a 5-10 mm long piece of the nerve trunk (Zigmond et al., 1985). To denervate ECN targets, the ECN should be cut near the SCG and again more distally, removing a 3-5 mm long piece of the nerve (Romeo et al., 1986). Finally, to denervate ICN targets, the ICN should be cut near its entry into the carotid canal and again near the SCG, removing a piece of 3-5 mm of the nerve (Zigmond et al., 1985).

15. When a bilateral SCGx is to be performed, repeat the procedure on the other side of the neck.

16. Pull out the self-retaining retractor.

Closure and postoperative care

17. Close the skin with 4-0 nylon, using a simple interrupted suture, placing a stitch every 4-5 mm. Skin can be also closed using wound clips.

18. Wipe the skin with povidone-iodine solution.

19. Place the rat on a warming pad to recover.

20. Transfer the animal into a cage with free access to food and water in a warm and stress free environment.

▲**CRITICAL STEP** Rats with bilateral SCGx barely survive in a cold environment (<16ºC) within the first 48 hours post-surgery. Moreover, acute SCGx produces a mild nocturnal hypothermia. Rats return to their preoperative baseline levels of body temperature around the second day after SCGx (Romeo et al., 2009).

! CAUTION Denervated tissues may respond to systemic catecholamines released by the adrenal medulla under stress conditions, complicating data interpretation (Klein et al., 1971; Parfitt and Klein, 1976; Lynch et al., 1977). Loss of neuronal NE uptake sites in presynaptic membranes which accompanies the degeneration of the sympathetic nerve terminals and upregulation of NE receptors in the postsynaptic membranes may cause supersensitivity to circulating catecholamines in denervated organs (Iversen, 1971; Zigmond et al., 1985).

? TROUBLESHOOTING

Troubleshooting advice can be found in Table 1.

Complete recovery of the rat is expected about one hour after the end of the surgery when ketamine/xylazine anesthesia is used. Due to the anatomical

characteristics of the cervical region, the risk of inadvertent damage to neural structures other than the SCG and its branches is minimal, and no vascular injury should occur when the surgical technique described here is carefully followed. However, if the CBA is accidentally damaged during surgical manipulation, profuse bleeding will occur, and hypoxia/ischemia effects on the ganglia are to be expected (Santer and Owen, 1986).

Operators with basic surgery skills can expect a learning curve of ~20 animals to efficiently perform the SCGx. One of the coauthors, who had no previous surgical training in SCGx (M.R.F.), was able to master this technique by closely following this protocol. After an initial training period, the expected perioperative mortality using the innovative technique should be near 0%, and bilateral SCGx should take ~15 minutes.

3.3. Verification of surgical performance

3.3.1. Blepharoptosis

The palpebral ptosis is used as indicator of the successful removal of the SCG (Fig. 3A). Based on the Wallerian anterograde degeneration paradigm (latency-activation-paralysis), this phenomenon presents a specific time sequence: 1) transient blepharoptosis after the effects of the anesthetic wear off, up to ~10 hours post-SCGx; 2) transitory exophthalmus (protrusion of the eyeball) from ~10 to 30 hours after SCGx (Fig. 3B); 3) irreversible blepharoptosis from ~30 hours on. Animals without bilateral palpebral ptosis and, therefore, with incomplete surgery, could be easily identified and discarded.

3.3.2. Histology

A histological study of the removed structure is recommended to validate the success of the SCGx, especially during the early training phase. The macroscopic features of the SCG are shown in Figure 3D. Using classic staining techniques, different neuronal populations surrounded by satellite cells and crossed fibers were identified. The presence of an undisrupted connective tissue capsule and the proximal stumps of the pre and postganglionic nerves did confirm the complete harvesting of the SCG. Immunohistochemical studies were performed to corroborate the neuronal and sympathetic nature of the SCG *via* identification of neurofilaments and the enzyme tyrosine hydroxilase, respectively (Figs. 3E-F).

4. Discussion

During the last decades, the SCGx has become a reliable model in neuroscience, especially in neurophysiology, homeostatic regulation and neural recovery and regeneration after injury. In addition to the key location of the SCG in the sympathetic chain and their well-defined field of innervation, several anatomical and physiological features explain the breadth of application of this surgical procedure. In rat, the removal of the SCG can be performed through a minimally invasive approach with very low morbimortality rates. Moreover, the well-characterized anatomy of the SCG allows the operator to effect, with high reliability and reproducibility, different disruptions of the sympathetic pathway using the same surgical approach. It is possible to perform: 1) SCGx; 2) decentralization by cervical ST lesion (lesion of preganglionic axons) (STx) and; 3) denervation *via* ICN or ECN lesion (lesion of postganglionic axons) (ICNx and ECNx). Notably, each procedure causes distinct physiological impacts. Whereas the SCGx removes all the neuronal cell bodies leading a complete and irreversible sympathetic denervation, a STx leaves the undamaged ganglia *in situ,* preserving neuronal responsiveness to hormonal and cytokine input signals and maintaining physiological activities in the postganglionic nerve endings, such as NE uptake (Iversen, 1971; Klein and Parfitt, 1976). The latter physiological mechanism makes decentralization a more effective procedure to completely prevent adrenergic stimulation in target tissues, such as the pineal gland, since the surviving nerve terminals from SCG postganglionic neurons will take up and inactive circulating catecholamines released under stress (Parfitt and Klein, 1976; Zigmond et al., 1985). On the other hand, the lesion of postganglionic axons unleashes a transitory sympathetic interruption, since the

injured neurons inside the SCG form regenerative sprouts that may reinnervate the denervated tissues and organs leading to variable recovery (Bowers et al., 1984). The animal`s age and gender, the nature of injury, the distance between the lesion and the pericaryon, and the time frame between surgery and the analysis of its effects are all factors for consideration in choosing the model (Barron, 1983; Taxi and Eugène, 1995).

The possibility of performing different reproducible lesions and measuring quantitatively the degree of functional disruption and recovery through markers such as AA-NAT and melatonin makes SCG-related procedures ideal models to study the morphological, biochemical and physiological alterations of damaged neurons. Furthermore, the bilateral distribution of the SCG allows the combination of different SCG-related procedures in the same animal. In overlapping innervation target fields, such as the pineal gland, it is possible to perform unilateral procedures to study compensatory changes in the contralateral sympathetic pathway. On the other hand, when a structure is only innervated by the ipsilateral SCG, the contralateral target organ may be used as a control after a unilateral lesion.

As previously mentioned, SCGx implies the ablation of neuronal cell bodies that project their axons through the carotid nerves, activating the mechanisms responsible for anterograde degeneration. The resulting dual phenomenon of sympathetic inhibition and excitation makes the SCGx has advantages compared to electrical stimulation of the ST, which requires an anesthetized animal during assessment of outcome, and chemical sympathectomy. The latter, which is a commonly used strategy in chronic sympathetic denervation studies (Picklo, 1997), may induce several side effects

and autonomic systemic reflex sequelae, and unexpected toxic effects may lead to increased morbimortality rates. In addition, the degree of sympathetic depletion is dose-dependent, and evidence suggests that some drugs are not capable of sufficiently disrupting noradrenergic influence in specific target tissues, e.g. guanethidine in the rat pineal gland (Reuss and Kreis, 1995).

Palpebral position is a useful indicator of the time course of nerve degeneration and, therefore, the phase of the sympathetic inhibition/excitation phenomenon after SCG removal (Cardinali and Romeo, 1991) (Table 2). During the latent phase and chronic SCGx, NE is not released from the synaptic buttons at the Müller's muscle. In consequence, this muscle becomes weak, leading to blepharoptosis. During acute SCGx, a transitory supraliminal release of NE from the degenerating varicosities may cause a sympathetic overstimulation of the extraocular and palpebral muscles, leading to palpebral retraction and eye ball protrusion (exophthalmus).

Blepharoptosis is the most common sign after SCGx and usually the only one used to assess the effectiveness of the surgery. Nevertheless, blepharoptosis itself does not necessarily imply that the SCG were completely removed. Either SCGx, STx or ICNx disrupt the sympathetic pathway to the eye, leading to eyelid ptosis. In our experience, when the classical technique is used, an incomplete SCG ablation or the section of the ST and/or ICN during removal of other tissues (e.g. fat, lymph node, muscle) instead the ganglia are the most frequent causes of false-positive ptosis. A conscientious evaluation of the time-dependent palpebral phenomenon may help to identify these mistakes, common in the early training phase, and discard the animals. This strategy exploits the lack of the exophthalmus phase in those animals where the ST

were sectioned but the SCG neurons were not damaged; that is, when the anterograde degeneration of the ICN axons did not occur.

Blepharoptosis must be evaluated in an absolutely calm animal, otherwise systemic catecholamine release into the bloodstream due to stress may cause eyelid retraction in a properly ganglionectomized animal, resulting in a false-negative error. On the other hand chromodacryorhoea, a red periocular staining, may be occasionally seen during the first 72 hours post-SCGx due to the excessive porphyrin production by the rat Harderian gland (Fig. 3C). If this event persists, the presence of infectious diseases in the animal facility should be investigated (Williams, 2002).

To the best of our knowledge this manuscript presents the first thorough description of the SCGx in rat in the literature. An innovative procedure to reach and remove the SCG without muscular injury is also introduced here. This new strategy makes SCGx a more precise, less invasive and highly reproducible model. Moreover, the innovative technique allows the operator to confirm a complete ablation of the SCG and the proximal stumps of the emerging nerves during surgery. Advantages and disadvantages of the classical and innovative techniques can be found in Table 3.

The anatomical study presented here is consistent with previous descriptions of the cervical sympathetic chain (Hedger and Webber,1976; Weijnen *et al*.,2000) and the arterial vessels of the upper neck (Santer and Owen, 1986). Our additional contribution is to describe the anatomical-surgical layers of the ventral neck, emphasizing the anatomical landmarks to reach the SCG and to identify their principal branches to consistently perform different SCG-related procedures.

In conclusion, this paper provides a review of the principal features and applications of the SCGx, presents valuable anatomical landmarks in the rat's neck, describes in detail, for the first time in the literature, two alternative surgical procedures to completely remove the SCG, and offers visual material for training purposes. We hope that standardization of the rat SCGx protocol will allow researchers to organize knowledge into a cohesive framework in the different areas where the SCGx is applied.

Acknowledgments

We thank Bruno Valente and Franco Pellegrino for helping with the production of the video, Dr. Cristina Semino-Mora for providing an optimized immunohistochemical protocol, and Dr. Sean Ingram Patterson for correcting the English. We thank Dr. Bobbie Ann Austin for editing and reviewing the manuscript. L.E.S., A.E.C., M.R.F., H.E.R. and E.M.M. are supported by CONICET, ANPCyT and MINCyT(Argentina)-CONICYT(Chile) (PICT-CONICET 2007-682 and CH/09/10 to E.M.M.; PIP-CONICET 114-20080100100 to H.E.R). M.F.R. is supported by The Danish Medical Research Council. L.E.S. and M.R.F. are recipients of research fellowships from the School of Medicine and National University of Cuyo. The anti-neurofilament and anti-tyrosine hydroxylase antibodies were kindly provided by Dr. Miguel Concha (Laboratorio de Estudios Ontogénicos, Programa de Anatomía y Biología del Desarrollo, ICBM, Facultad de Medicina, Universidad de Chile) and Dr. Matias Pandolfi (Departamento de Biodiversidad y Biología Experimental, Facultad de Ciencias Exactas y Naturales, Universidad de Buenos Aires), respectively. The authors declare that they have no competing financial interests.

References

Bäckström M, Olson L, Seiger A. N-acetyltransferase and hydroxyindole-O-methyltransferase activity in intraocular pineal transplants: diurnal rhythm as evidence for functional sympathetic adrenergic innervation. Acta Physiol Scand 1976;96:64-71.

Barron KD. Comparative observations on the cytologic reactions of the central and peripheral nerve cells to axotomy. Kao CC, Bunge RP, Reier PJ, editors. Spinal Cord Reconstruction. Raven Press: New York, 1983;7-40.

Benarroch EE. Neuropeptides in the sympathetic system: presence, plasticity, modulation, and implications. Ann Neurol 1994;36:6-13.

Boggio V, Ladizesky MG, Cutrera RA, Cardinali DP. Autonomic neural signals in bone: physiological implications for mandible and dental growth. Life Sci 2004;75:383-95.

Borjigin J, Wang MM, Snyder SH. Diurnal variation in mRNA encoding serotonin N-acetyltransferase in pineal gland. Nature 1995;378:783-5.

Bowers CW, Baldwin C, Zigmond RE. Sympathetic reinnervation of the pineal gland after postganglionic nerve lesion does not restore normal pineal function. J Neurosci 1984;4:2010-5.

Cardinali DP, Romeo HE. The autonomic nervous system of the cervical region as a channel of neuroendocrine communication. Front Neuroendocrinol 1991;12:278-97.

Cardinali DP, Stern JE. Peripheral neuroendocrinology of the cervical autonomic nervous system. Braz J Med Biol Res 1994;27:573-99.

Cavallotti C, Frati A, Sagnelli P, Pescosolido N. Re-evaluation and quantification of the different sources of nerve fibres supplying the rat eye. J Anat 2005;206:217-24.

Coutard M, Mertes P, Mairose P, Osborne-Pellegrin M, Michel JB. Arterial sympathetic innervation and cerebrovascular diseases in original rat models. Auton Neurosci 2003;104:137-45.

Elenkov IJ, Wilder RL, Chrousos GP, Vizi ES. The sympathetic nerve--an integrative interface between two supersystems: the brain and the immune system. Pharmacol Rev 2000;52:595-638.

Emmelin N, Trendelenburg U. Degeneration activity after parasympathetic or sympathetic denervation. Ergeb Physiol 1972;66:147-211.

Esquifino AI, Cardinali DP. Local regulation of the immune response by the autonomic nervous system. Neuroimmunomodulation 1994;1:265-73.

Gibbs GF, Drummond PD, Finch PM, Phillips JK. Unravelling the pathophysiology of complex regional pain syndrome: focus on sympathetically maintained pain. Clin Exp Pharmacol Physiol 2008;35:717-24.

Haug SR, Heyeraas KJ. Modulation of dental inflammation by the sympathetic nervous system. J Dent Res 2006;85:488-95.

Hedger JH, Webber RH. Anatomical study of the cervical sympathetic trunk and ganglia in the albino rat (Mus norvegicus albinus). Acta Anat 1976;96:206-17.

Ifft JD. The effect of superior cervical ganglionectomy on the cell population of the rat adenohypophysis and on the estrous cycle. Anat Rec 1953;117:395-404.

Iversen LL. Role of transmitter uptake mechanisms in synaptic neurotransmission. Br J Pharmacol 1971;41:571-91.

Jänig W, Häbler HJ. Neurophysiological analysis of target-related sympathetic pathways--from animal to human: similarities and differences. Acta Physiol Scand 2003;177:255-74.

Klein DC, Weller JL, Moore RY. Melatonin metabolism: neural regulation of pineal serotonin: acetyl coenzyme A N-acetyltransferase activity. Proc Natl Acad Sci U S A 1971;68:3107-10.

Klein DC, Parfitt A. A protective role of nerve endings in the stress-stimulated increase in pineal N-acetyltransferase activity. Kvetnansky R, Usdin E, editors. Catecholamines and Stress. Pergamon Press: New York, 1976;119-28.

Klein DC. Arylalkylamine N-acetyltransferase: "the Timezyme". J Biol Chem 2007;282:4233-7.

Klimaschewski L, Kummer W, Heym C. Localization, regulation and functions of neurotransmitters and neuromodulators in cervical sympathetic ganglia. Microsc Res Tech 1996;35:44-68.

Lingappa JR, Zigmond RE. Pineal transplants in oculo: limitations on the ability of collateral sprouts of foreign neurons to establish normal function. J Neurosci 1987;7:3525-8.

Lynch HJ, Ho M, Wurtman RJ. The adrenal medulla may mediate the increase in pineal melatonin synthesis induced by stress, but not that caused by exposure to darkness. J Neural Transm 1977;40:87-97.

Mathison R, Davison JS, Befus AD. Neuroendocrine regulation of inflammation and tissue repair by submandibular gland factors. Immunol Today 1994;15:527-32.

Maronde E, Stehle JH. The mammalian pineal gland: known facts, unknown facets. Trends Endocrinol Metab 2007;18:142-9.

May A, Goadsby PJ. The trigeminovascular system in humans: pathophysiologic implications for primary headache syndromes of the neural influences on the cerebral circulation. J Cereb Blood Flow Metab 1999;19:115-27.

Møller M, Phansuwan-Pujito P, Morgan KC, Badiu C. Localization and diurnal expression of mRNA encoding the beta1-adrenoceptor in the rat pineal gland: an in situ hybridization study. Cell Tissue Res 1997;288:279-84.

Møller M, Baeres FM. The anatomy and innervation of the mammalian pineal gland. Cell Tissue Res 2002;309:139-50.

Moore RY, Klein DC. Visual pathways and the central neural control of a circadian rhythm in pineal serotonin N-acetyltransferase activity. Brain Res 1974;71:17-33.

Moore RY. Pineal transplants to the anterior chamber of the eye: evidence for functional reinnervation. Exp Neurol 1975;49:617-21.

Muñoz EM, Bailey MJ, Rath MF, Shi Q, Morin F, Coon SL, Møller M, Klein DC. NeuroD1: developmental expression and regulated genes in the rodent pineal gland. J Neurochem 2007;102:887-99.

Nagao T, Sadoshima S, Ishitsuka T, Kusuda K, Shiokawa O, Ibayashi S, Fujishima M. Effects of acute superior cervical ganglionectomy on cerebral blood flow and metabolism in stroke-prone spontaneously hypertensive rats subjected to cerebral ischaemia. Clin Exp Pharmacol Physiol 1992;19:489-93.

Nance DM, Sanders VM. Autonomic innervation and regulation of the immune system (1987-2007). Brain Behav Immun 2007;21:736-45.

Parfitt AG, Klein DC. Sympathetic nerve endings in the pineal gland protect against acute stress-induced increase in N-acetyltransferase (EC 2.3.1.5.) activity. Endocrinology 1976;99:840-51.

Perl ER. Causalgia, pathological pain, and adrenergic receptors. Proc Natl Acad Sci U S A 1999;96:7664-7.

Perreau-Lenz S, Kalsbeek A, Garidou ML, Wortel J, van der Vliet J, van Heijningen C, Simonneaux V, Pévet P, Buijs RM. Suprachiasmatic control of melatonin synthesis in rats: inhibitory and stimulatory mechanisms. Eur J Neurosci 2003;17:221-8.

Perreau-Lenz S, Kalsbeek A, Van Der Vliet J, Pévet P, Buijs RM. In vivo evidence for a controlled offset of melatonin synthesis at dawn by the suprachiasmatic nucleus in the rat. Neuroscience 2005;797-803.

Picklo MJ. Methods of sympathetic degeneration and alteration. J Auton Nerv Syst 1997;62:111-25.

Raju B, Haug SR, Ibrahim SO, Heyeraas KJ. Sympathectomy decreases size and invasiveness of tongue cancer in rats. Neuroscience 2007;149:715-25.

Ramaswamy K, Mathison R, Carter L, Kirk D, Green F, Davison JS, Befus D. Marked antiinflammatory effects of decentralization of the superior cervical ganglia. J Exp Med 1990;172:1819-30.

Rath MF, Muñoz E, Ganguly S, Morin F, Shi Q, Klein DC, Møller M. Expression of the Otx2 homeobox gene in the developing mammalian brain: embryonic and adult expression in the pineal gland. J Neurochem 2006;97:556-66.

Rath MF, Bailey MJ, Kim JS, Ho AK, Gaildrat P, Coon SL, Møller M, Klein DC. Developmental and diurnal dynamics of Pax4 expression in the mammalian pineal gland: nocturnal down-regulation is mediated by adrenergic-cyclic adenosine 3',5'-monophosphate signaling. Endocrinology 2009;150:803-11.

Reuss S, Moore RY. Neuropeptide Y-containing neurons in the rat superior cervical ganglion: projections to the pineal gland. J Pineal Res 1989;6:307-16.

Reuss S, Kreis T. Pineal 'synaptic' ribbon numbers and melatonin synthesis of rat are resistant to guanethidine sympathectomy. Experientia 1995;51:332-4.

Ribeiro AA, Davis C, Gabella G. Estimate of size and total number of neurons in superior cervical ganglion of rat, capybara and horse. Anat Embryol 2004;208:367-80.

Romeo HE, González Solveyra C, Vacas MI, Rosenstein RE, Barontini M, Cardinali DP. Origins of the sympathetic projections to rat thyroid and parathyroid glands. J Auton Nerv Syst 1986;17:63-70.

Romeo HE, Spinedi E, Vacas MI, Estivariz F, Cardinali DP. Increase in adrenocorticotropin release during wallerian degeneration of peripheral sympathetic neurons after superior cervical ganglionectomy of rats. Neuroendocrinology 1990;51:213-8.

Romeo HE, Arias P, Szwarcfarb B, Moguilevsky JA, Cardinali DP. Hypothalamic luteinizing hormone-releasing hormone content and serum luteinizing hormone levels in male rats during wallerian degeneration of sympathetic nerve terminals after superior cervical ganglionectomy. J Neural Transm Gen Sect 1991a;85:41-9.

Romeo HE, Colombo LL, Esquifino AI, Rosenstein RE, Chuluyan HE, Cardinali DP. Slower growth of tumours in sympathetically denervated murine skin. J Auton Nerv Syst 1991b;32:159-64.

Romeo HE, Fink T, Yanaihara N, Weihe E. Distribution and relative proportions of neuropeptide Y- and proenkephalin-containing noradrenergic neurones in rat superior cervical ganglion: separate projections to submaxillary lymph nodes. Peptides 1994;15:1479-87.

Romeo HE, Tio DL, Taylor AN. Effects of superior cervical ganglionectomy on body temperature and on the lipopolysaccharide-induced febrile response in rats. J Neuroimmunol 2009;209:81-6.

Roseboom PH, Coon SL, Baler R, McCune SK, Weller JL, Klein DC. Melatonin synthesis: analysis of the more than 150-fold nocturnal increase in serotonin N-acetyltransferase messenger ribonucleic acid in the rat pineal gland. Endocrinology 1996;137:3033-45.

Santer RM, Owen RG. Arterial supply of the rat superior cervical ganglion: a morphological and semiquantitative histochemical investigation. J Anat 1986;147:107-14.

Semino-Mora C, Doi SQ, Marty A, Simko V, Carlstedt I, Dubois A. Intracellular and interstitial expression of Helicobacter pylori virulence genes in gastric precancerous intestinal metaplasia and adenocarcinoma. J Infect Dis 2003;187:1165-77.

Smolen AJ, Wright LL, Cunningham TJ. Neuron numbers in the superior cervical sympathetic ganglion of the rat: a critical comparison of methods for cell counting. J Neurocytol 1983;12:739-50.

Stehle JH, Foulkes NS, Molina CA, Simonneaux V, Pévet P, Sassone-Corsi P. Adrenergic signals direct rhythmic expression of transcriptional repressor CREM in the pineal gland. Nature 1993;365:314-20.

Taxi J, Eugène D. Effects of axotomy, deafferentation, and reinnervation on sympathetic ganglionic synapses: a comparative study. Int Rev Cytol 1995;159:195-263.

Wasner G, Schattschneider J, Binder A, Baron R. Complex regional pain syndrome--diagnostic, mechanisms, CNS involvement and therapy. Spinal Cord 2003;41:61-75.

Weaver DR. The suprachiasmatic nucleus: a 25-year retrospective. J Biol Rhythms 1998;13:100-12.

Weijnen JA, Surink S, Verstralen MJ, Moerkerken A, De Bree GJ, Bleys RL. Main trajectories of nerves that traverse and surround the tympanic cavity in the rat. J Anat 2000;197:247-62.

Williams DL. Ocular disease in rats: a review. Vet Ophthalmol 2002;5:183-91.

Wragg LE, Machado CR, Snyder SH, Axelrod J. Anterior chamber pineal transplants: their metabolic activity and independence of environmental lighting. Life Sci 1967;6:31-8.

Wu W, Scott DE, Reiter RJ. Transplantation of the mammalian pineal gland: studies of survival, revascularization, reinnervation, and recovery of function. Exp Neurol 1993;122:88-99.

Yamazaki S, Yoshikawa T, Biscoe EW, Numano R, Gallaspy LM, Soulsby S, Papadimas E, Pezuk P, Doyle SE, Tei H, Sakaki Y, Block GD, Menaker M. Ontogeny of circadian organization in the rat. J Biol Rhythms 2009;24:55-63.

Zigmond RE, Baldwin C, Bowers CW. Rapid recovery of function after partial denervation of the rat pineal gland suggests a novel mechanism for neural plasticity. Proc Natl Acad Sci U S A 1981;78:3959-63.

Zigmond RE, Baldwin C, Bowers CW. Rapid recovery of pineal function after partial denervation: a possible role for heteroneuronal uptake of transmitter in modulating synaptic efficacy. J Neurosci 1985;5:142-50.

Zigmond RE. Neuropeptide action in sympathetic ganglia. Evidence for distinct functions in intact and axotomized ganglia. Ann N Y Acad Sci 2000;921:103-8.

Figure 1 | Photo series of the dissection of an exsanguinated rat's neck. **(A)** Ventral view of the neck with key anatomical landmarks. **(B)** Exposure of the superficial cervical fascia (SCF) after retracting the skin. **(C)** Removal of the SCF and exposure of the mandibular glands, Wharton`s ducts, anterior belly of the digastric muscles (aDM), masseter muscles (MM), external jugular veins (EJV) and lymph nodes. **(D)** Retraction of both mandibular glands and complete visualization of the left EJV. SMM: sternomastoid muscles. **(E)** Exposure of the SMM, sternohyoid (SHM) and omohyoid muscles (OHM), aDM and posterior belly of the digastric muscle (pDM). The boundary between the SHM and the left OHM is indicated with a dotted black line. **(F)** Retraction of the left SMM and exposure of the carotid triangle (CT). **(G)** Transection of the left OHM and SMM and exposure of the deep cervical fascia (DCF), the carotid sheath and lymph nodes. The carotid bifurcation zone is located below and medially from the mandibular angular process. **(H)** Partial removal of the left carotid sheath and medialization of the external carotid artery (ECA). The common carotid artery (CCA), vagus nerve (VN), the carotid bifurcation into ECA and internal carotid artery (ICA), the occipital artery (OA) and the hypoglossal nerve (HN) are clearly observed. The SCG is located behind the carotid bifurcation and is still embedded in fat and connective tissue. **(I)** Removal of the left OA and dissection of the SCG, external and internal carotid nerves (ECN and ICN) and the sympathetic trunk (ST).

Figure 2 | Strategies to reach and identify the SCG. **(A)** Image of the rat neck ventral area showing the *regio presternalis*, the *regio intermandibularis* between the mandibular branches, and the line where the skin incision will be performed (dotted black line). **(B)** Exposure of the superficial cervical fascia (SCF) after skin incision. **(C)** Retraction of the skin's cut edges and exposure of the branches of the external jugular veins (EJV). The boundaries of the mandibular glands are indicated with dotted black ovals. A dotted line indicates the place where the SCF will be cut. **(D)** Exposure of the sternohyoid (SHM) and sternomastoid (SMM) muscles, and the EJV after retraction of the mandibular glands. Dotted black ovals indicate the beating areas. Inset: branches of the linguofacial veins (LFV) and Wharton's duct. **(E)** The dotted black line on the right side of the neck shows where the omohyoid muscle (OHM) will be transected in the classical technique. On the left side, the carotid triangle (CT), the anatomical landmark used in the innovative technique, is fully exposed after cutting the connective tissue sheets that bind together the SHM and the posterior belly of the DM (pDM) (see inset). The SMM, the pDM and the partially exposed OHM compose the boundaries of the CT, which is covered by the deep cervical fascia (DCF). **Classical technique: (F)** Transection of the OHM and retraction of its cut edges with Q-tips, revealing the common carotid artery (CCA) and the vagus nerve (VN). Inset: the SCG, covered by connective tissue, is observed underneath the carotid bifurcation into external and internal carotid arteries (ECA and ICA) and the occipital artery (OA), and medially from the hypoglossal nerve (HN). **(G)** Exposure of the SCG after pulling the ECA laterally (see inset). **Innovative technique: (F')** Identification of the CCA, ECA, ICA, HN and SCG through the CT (see inset). **(G')** Exposure of the SCG by pulling

laterally on the ECA. Note that the artery is held indirectly by the DCF (see inset). **(H)** Outcome after bilateral SCGx using the classical (right) and the innovative (left) techniques. Muscle injury is not caused in the latter approach.

Figure 3 | Verification of surgical performance. **(A)** Unilateral blepharoptosis after left superior cervical ganglionectomy (SCGx). **(B)** Transient unilateral exophthalmus after left SCGx. **(C)** Chromodacryorhoea after bilateral SCGx. **(D)** Macroscopic view of the superior cervical ganglion (SCG) and its pre and postganglionic branches. ST: sympathetic trunk; ECN and ICN: external and internal carotid nerves. Scale bar: 2 mm. **(E)** Indirect immunohistochemistry revealing neurofilament-containing cells within the SCG (green, 10X). Inset: fluorescent neurofilaments and DAPI-labeled nuclei (blue, 60X). Scale bar: 0.5 mm. **(F)** Immunohistochemistry showing the sympathetic nature of the SCG via labeling tyrosine hydroxylase-containing neurons (red, 10X). Inset: fluorescent sympathetic perikarya with a cytoplasmic granular pattern and DAPI-labeled nuclei (blue, 60X). Scale bar: 0.5 mm.

TABLE 1 | Troubleshooting table.

Step	Problem	Possible Reason	Solution
11	Salivary gland' damage and bleeding	Unclear boundary between right and left mandibular glands	Stretch the superficial cervical fascia and cut the poorly vascularized connective tissue following the neck`s midline
14. Classical Technique. A.i	Poor exposure of the beating area	Inadequate omohyoid muscle exposure	Retract skin and salivary glands completely and retract the sternomastoid and sternohyoid muscles laterally and medially, respectively
14. Classical Technique. A.iv	Carotid bifurcation is not identified	Carotid bifurcation is covered by the deep cervical fascia	Remove the deep cervical fascia using microdissecting tweezers
		Internal carotid artery is barely seen due to its deeper and lateral location	Bluntly dissect the common carotid artery until its Y-shaped bifurcation is identified
14. Classical Technique. B.ii	SCG is not found	Insufficient traction of the external carotid artery	Pull the external carotid artery further
		Surgical field is blood-stained	Wipe out blood with a Q-tip
14. Innovative Technique. A.	Carotid triangle is not identified	Sternohyoid muscle and posterior belly of the digastric muscle are bound by the deep cervical fascia	Cut the connective tissue sheets between both muscles and, with Q-tips, simultaneously push the sternohyoid and omohyoid muscles medially and the posterior belly of the digastric muscle laterally
		Carotid triangle is masked by a lymph node	Displace the lymph node

TABLE 2 | The SCGx paradigm and blepharoptosis.

Neuronal modifications	Experimental phase	Onset and duration	Neurotransmitter release	Norepinephrine levels in the denervated organs	Effects	Upper eyelid position
Perikarya removal (SCGx)	Latency phase	0 to 10h	Not present	Stable concentration	Transitory postsynaptic paralysis	Transient blepharoptosis
Wallerian degeneration	Acute SCGx	10 to 30h	Supraliminal release from the degenerating varicosities	Progressive decrease	Postsynaptic activation	Temporary exophthalmus
Complete nerve degeneration	Chronic SCGx	>30h	Not present	Complete norepinephrine depletion	Permanent postsynaptic paralysis	Permanent blepharoptosis

TABLE 3 | Classical *vs.* innovative techniques: advantages and disadvantages.

	CLASSICAL TECHNIQUE	INNOVATIVE TECHNIQUE
Muscular section (Fig. 1h)	Required	Not required
Use of the carotid triangle as a key anatomical landmark	No	Yes
Risk of massive bleeding due to artery tear*	Medium-Low	Very Low
Animal mortality*	Medium-Low	Very Low
Risk of incomplete SCG removal*	Medium	Very low[#]
Surgical skills, anatomical knowledge and experience	Less required	More required

***These outcomes are strongly operator and training phase-dependent.
[#] Intact ganglion harvesting allows further studies on the removed SCG.

Figure 1

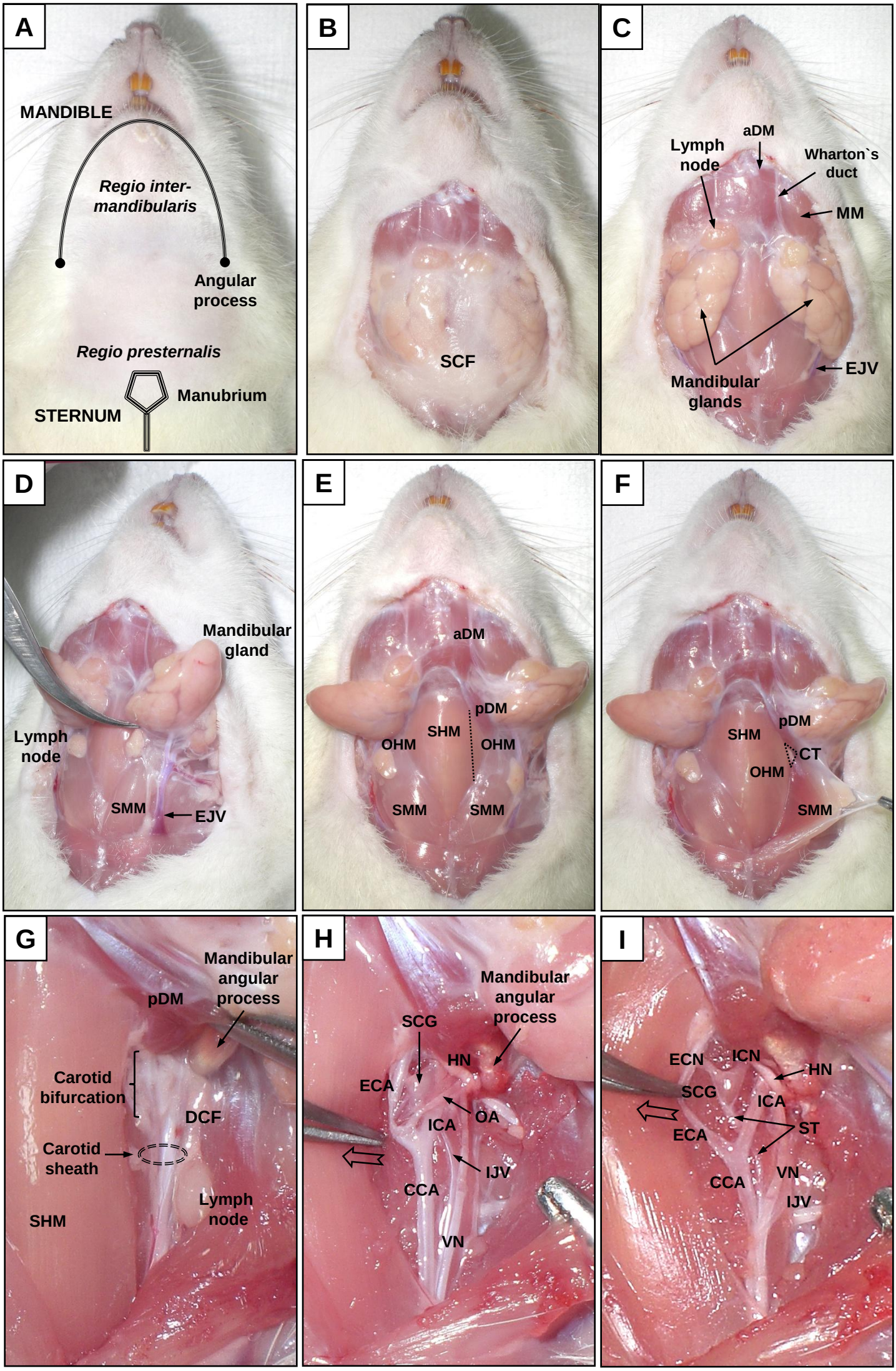
A
MANDIBLE
Regio inter-
mandibularis
Angular
process
Regio presternalis
STERNUM
Manubrium
B
SCF
C
Lymph
node
aDM
Wharton`s
duct
MM
EJV
Mandibular
glands
D
Mandibular
gland
Lymph
node
SMM
EJV
E
aDM
pDM
SHM
OHM
OHM
SMM
SMM
F
pDM
SHM
CT
OHM
SMM
G
Mandibular
angular
process
pDM
Carotid
bifurcation
DCF
Carotid
sheath
Lymph
node
SHM
H
Mandibular
angular
process
SCG
HN
ECA
OA
ICA
IJV
CCA
VN
I
ECN
ICN
HN
SCG
ICA
ECA
ST
CCA
VN
IJV

Figure 2

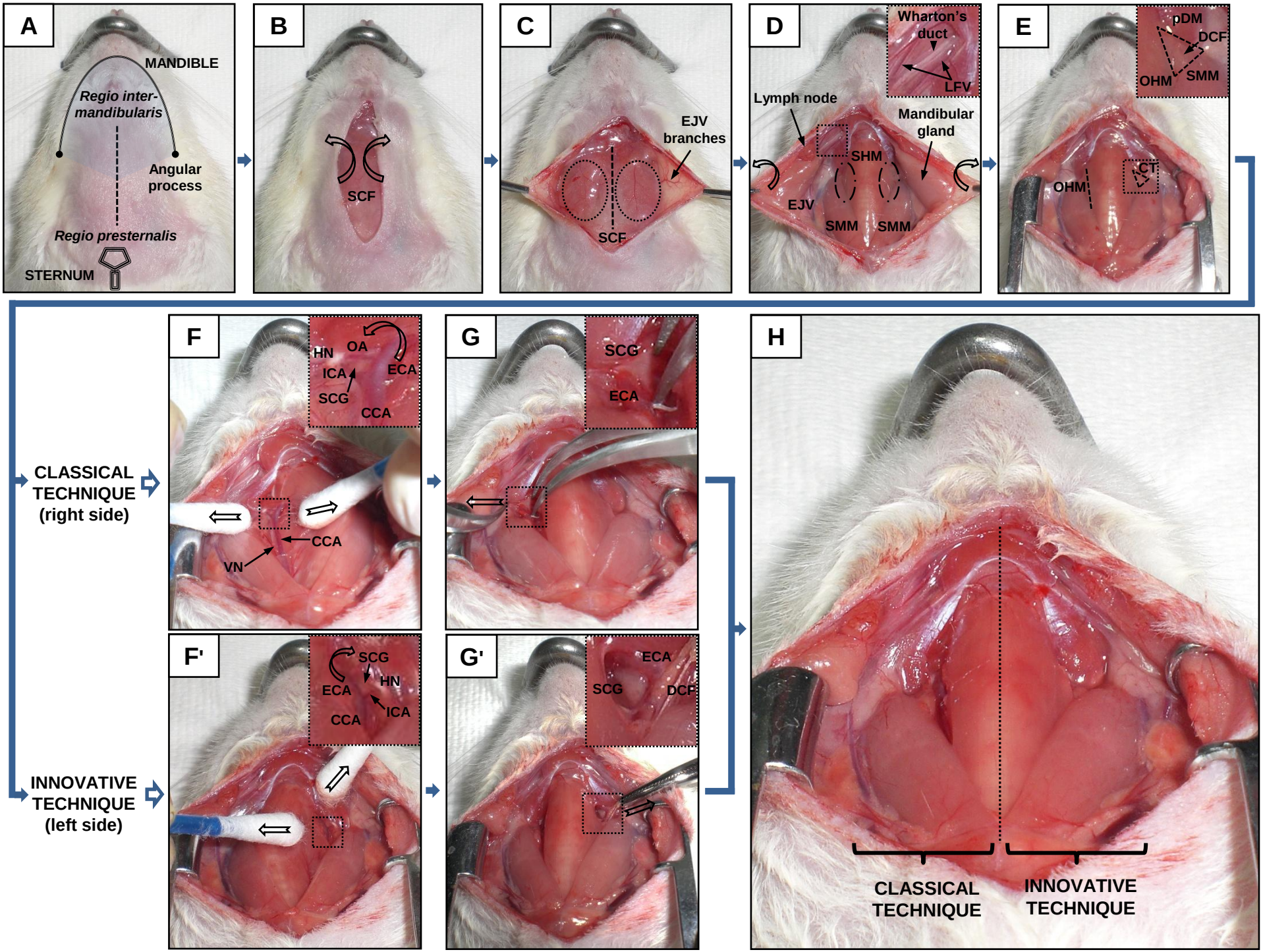
A
MANDIBLE
Regio inter-mandibularis
Angular process
Regio presternalis
STERNUM
B
SCF
C
EJV branches
SCF
D
Wharton's duct
LFV
Lymph node
Mandibular gland
SHM
EJV
SMM
SMM
E
pDM
DCF
OHM
SMM
CT
OHM
CLASSICAL TECHNIQUE (right side)
INNOVATIVE TECHNIQUE (left side)
F
HN
OA
ICA
ECA
SCG
CCA
CCA
VN
G
SCG
ECA
F'
SCG
ECA
HN
CCA
ICA
G'
ECA
SCG
DCF
H
CLASSICAL TECHNIQUE
INNOVATIVE TECHNIQUE

Figure 3

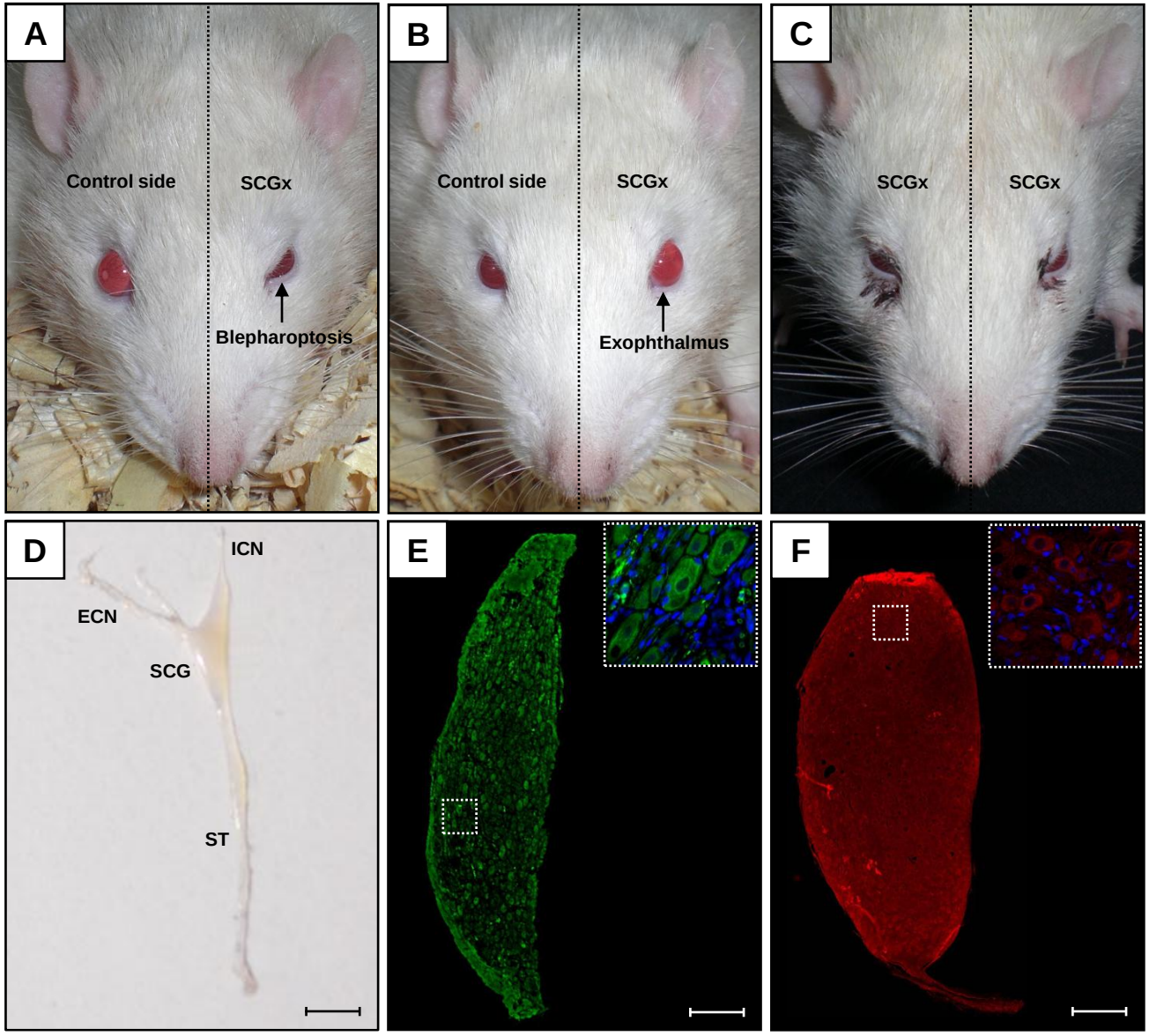
A
Control side
SCGx
Blepharoptosis
B
Control side
SCGx
Exophthalmus
C
SCGx
SCGx
D
ICN
ECN
SCG
ST
E
F